Virus-like particle preparation is improved by control over capsomere-DNA interactions during chromatographic purification

Lukas Gerstweiler[1], Jingxiu Bi[1], Anton Middelberg[2]

[1]The University of Adelaide, School of Chemical Engineering and Advanced Materials, SA 5000, Australia

[2]The University of Adelaide, Division of Research and Innovation

Correspodence concerning this article should be addressed to A.P.J. Middelberg at anton.middelberg@adelaide.edu.au

Abstract

Expression of viral capsomeres in bacterial systems and subsequent *in-vitro* assembly into virus-like particles is a possible pathway for affordable future vaccines. However, purification is challenging as viral capsomeres show poor binding to chromatography media. In this work, the behaviour of capsomeres in crude lysate was compared with that for purified capsomeres, with or without added microbial DNA, to better understand reasons for poor bioprocess behaviour. We show that aggregates or complexes form through the interaction between viral capsomeres and DNA, especially in bacterial lysates rich in contaminating DNA. The formation of these complexes prevents the target protein capsomeres from accessing the pores of chromatography media. We find that protein-DNA interactions can be modulated by controlling the ionic strength of the buffer and that at elevated ionic strengths the protein-DNA complexes dissociate. Capsomeres thus released show enhanced bind-elute behaviour on salt-tolerant chromatography media. DNA could therefore be efficiently removed. We believe this is the first report of the use of an optimised salt concentration that dissociates capsomere-DNA complexes yet enables binding to salt-tolerant media. Post purification, assembly experiments indicate that DNA-protein interactions can play a negative role during *in-vitro* assembly, as DNA-protein complexes could not be assembled into virus-like particles, but formed worm-like structures. This work reveals that the control over DNA-protein interaction is a critical consideration during downstream process development for viral vaccines.

Keywords

Modular virus-like particles, aggregation, DNA-protein interaction, downstream processing, multi modal chromatography

1. Introduction

Virus-like-particles (VLPs) are self-assembled ensembles of viral structural proteins, having the same size and shape as the native virus. However, as they lack viral nucleic acids, they cannot replicate and are therefore non-infectious. VLPs are able to trigger a strong immune response, due to their highly repetitive immunogenic and native structure, making them promising candidates as vaccines (Al-Barwani, Donaldson, Pelham, Young, & Ward, 2014; Bright et al., 2007; Donaldson, Lateef, Walker, Young, & Ward, 2018; Effio & Hubbuch, 2015; Hume et al., 2019). Vaccines based on VLPs are commercially available against Hepatitis B (HBV), Hepatitis E (HEV) and human papillomavirus (HPV). VLPs are currently investigated as vaccines against a variety of viruses such as Influenza A (IAV), human Norovirus (HuNV) and Chikungunya virus (Donaldson et al., 2018; Frazer, 2004; VBI Vaccines Inc, 2018).

By manipulating the amino acid sequence of the structural proteins, VLPs can be modified to present foreign antigens. In this way, they can trigger immune responses against others than the underlying virus. These so called modular VLPs do expand the possible applications of VLPs. Through synthetic biology, unrelated antigens can be presented in an immunogenic context, allowing multivalent and cross protective vaccines to be generated against all kind of targets. As computer-based simulation is developing, these three dimensional structures can be precisely modelled to predict and obtain the desired immunogenicity and stability of the modular VLP (Mobini et al. 2020; Hume et al., 2019; Carter et al. 2016; Zhang, et al. 2015). Modular VLPs are examined as vaccines against pathogens like Group A Streptococcus (Seth et al., 2016), Influenza (Anggraeni et al., 2013), rotavirus (Tekewe, Fan, Tan, Middelberg, & Lua, 2017), human papillomavirus (Zhai et al., 2017) and also against malaria (Pattinson et al., 2019), toxoplasmosis (Guo et al., 2019), cancer (Donaldson et al., 2017), diabetes (Cavelti-Weder et al., 2016), nicotine addiction (Cornuz et al., 2008) and others.

Although VLPs are extremely promising as next-generation vaccines, large scale production is still a challenge (Hume et al., 2019; Pattenden, Middelberg, Niebert, & Lipin, 2005). Virus-like-particles can be produced by expressing viral structural protein in different host systems ranging from eukaryotics such as mammalian cells, yeast and insect cells to prokaryotic cell systems. Despite the usual pros and cons of these systems, namely post-translational modifications versus expression level and cost, the *in vivo* VLP self-assembly pathway always bears the risk of internal contaminations, like host cell DNA, RNA and host cell protein (HCP) that co-assemble together with VLPs. Internal contaminations are hard to remove and can lead to batch to batch variations (Lua et al., 2014; Pattenden et al., 2005; Teunissen, Raad, & Mastrobattista, 2013; Wu et al., 2010). The removal of internal contaminations requires an additional disassembling-reassembling step, including for the commercial HPV vaccine, making the overall process inefficient. Another pathway is the expression and purification of unassembled structural viral protein and a subsequent controlled *in vitro* assembly, eradicating the presence of internal contaminations and providing for enhanced process and product quality control (Pattenden et al., 2005).

Group A Streptococcus (GAS) is a human pathogen responsible for several million infections and more than 500,000 deaths every year (Carapetis, Steer, Mulholland, & Weber, 2005). An efficient vaccine has yet not been developed and only two candidates are being evaluated in human trials (Vekemans et al., 2019). As GAS is mainly a severe health problem in developing countries, an ideal future vaccine does not only have to be efficacious but also should be very affordable, as still more than 700 million people worldwide are living in extreme poverty (The World Bank, 2018; Wibowo, Chuan, Lua, & Middelberg, 2013). In this study a possible low-cost, future vaccine candidate, based on a modular polyoma virus-like-particle, was studied, that displays the J8 antigen from the GAS M-protein (Middelberg et al., 2011; Rivera-Hernandez et al., 2013).

The use of modified murine polyomavirus major capsid protein VP1 is a promising platform technology for fast, cheap and efficient modular VLP vaccines. It can be expressed in gram-

per-litre levels in *E. coli,* and produced within days, rather than months as most vaccines nowadays, enabling possible costs of cents per dose and potential for a fast reaction on pandemic outbreaks (Chuan, Wibowo, Lua, & Middelberg, 2014; Liew, Rajendran, & Middelberg, 2010; Middelberg et al., 2011). VP1 and VP1-derived proteins are highly examined to study self-assembling processes and the use of VLPs as drug carriers and vaccines (Chuan, Fan, Lua, & Middelberg, 2010; Li et al., 2003; Ou et al., 1999; Zhou et al., 2019). Like other viral proteins, the purification of VP1 capsomeres and VLPs presents challenges and no industrial scale process has yet been described (Buch et al., 2015; Gillock et al., 1997; Johne & Müller, 2004; Pattinson et al., 2019).

The main challenges during the purification of VP1 capsomeres and VLPs are low recoveries using chromatographic techniques (<40% on GSTrap™ HP affinity chromatography resins, 54% on CIMmultus™ QA monolith chromatography) and the formation of soluble aggregates during processing and assembling (Zayeckas et al. 2018; Lipin et al. 2008). Purification requires additional hard-to-scale unit operations, including size exclusion chromatography, enzymatic affinity tag removal or costly monoliths and membrane adsorbers (Zayeckas et al. 2018; Ladd Effio et al. 2016; Lipin et al. 2008). Also, DNA removal often requires additional enzymatic treatment (Simon et al. 2013). Aggregation and low recovery can influence each other as shown by Lipin et al. (2008), where low recovery on affinity chromatographic media could be attributed to the existence of aggregates unable to enter the pores of chromatographic resins.. Several mechanisms are proposed in the literature to cause aggregation, such as polymerisation by the used GST-tag, hydrophobic interactions, formation of disulphide bonds and a competitive pathway during assembly. Furthermore, the stability is highly dependent on the inserted antigen (Abidin, Lua, Middelberg, & Sainsbury, 2015; Ding, Chuan, He, & Middelberg, 2010; Lipin, Raj, Lua, & Middelberg, 2009; Tekewe, Connors, Middelberg, & Lua, 2016). It could be shown that capsomere stability can be increased by the addition of non-ionic detergents, sorbitol and polysorbate 20, and high-throughput methods have been developed to optimise buffer

composition (Abidin et al., 2015; Mohr, Chuan, Wu, Lua, & Middelberg, 2013; Tekewe et al., 2015).

Although the strong DNA binding properties of VP1 are a well-known fact and described decades ago (Chang, Cai, & Consigli, 1993; Moreland, Montross, & Garcea, 1991), the influence on aggregation and chromatographic purification has never been examined in detail. This study therefore explores the influence of VP1's DNA affinity on aggregation, chromatographic purification, protein stability and assembly. It is shown that VP1 aggregation (or complex formation), which hinders VP1 from accessing chromatography pores leading to poor binding capacities, can be caused by non-specific DNA-protein complexation, which can be eliminated by increasing salt concentration. Also, efficient strategies for chromatographic capture and the removal of nucleic acids are developed to overcome the bottleneck of producing VP1 based virus-like-particles. Furthermore, it was shown, that VP1-DNA complexes cannot be assembled into VLPs as they form worm like structures during assembly. The findings in this research are of high importance for the production of VP1 based virus-like-particles and will help to develop cheap and reliable industrial purification protocols.

2. Materials and methods

2.1 Chemicals and buffers

Cultivation was done with terrific broth (TB) medium containing 12 g l^{-1} tryptone (Thermo Fisher Scientific, USA), 24 g l^{-1} yeast extract (Thermo Fisher Scientific, USA), 5g l^{-1} glycerol (Chem-Supply, Australia), 2.31 g l^{-1} potassium dihydrogen phosphate (Chem-Supply, Australia) and 12.5 g l^{-1} dipotassium hydrogen phosphate (Chem-Supply, Australia). Chloramphenicol (Thermo Fisher Scientific, USA) and ampicillin (Thermo Fisher Scientific, USA) were added to final concentrations of 35 µg ml^{-1} and 100 µg ml^{-1}, respectively. IPTG for induction was obtained from Thermo Fisher Scientific, USA. Saline for cell resuspension

consisted of 9 g l^{-1} sodium chloride (Chem-Supply, Australia). Ultra-pure water was obtained with a Milli Q water (MQW) system and used for all experiments.

Lysis buffer comprised 40mM Tris buffer, 2mM EDTA, 5 % w w^{-1} glycerol and 5mM dithiothreitol (DTT) (all Chem-Supply, Australia) at pH 8. Lysis buffer without DTT was prepared as a 5X stock and prior use was filtered (0.22 µm), vacuum degassed for 5 min and DTT was added. For chromatographic experiments, lysis buffer containing different concentrations of NaCl were used. VLP assembling buffer consisted of 0.5 M ammonium sulphate, 20 mM Tris, 1mM calcium chloride and 5 % w w^{-1} glycerol (all Chem-Supply, Australia) at pH 7.4. Elution buffer at pH 12 was 40mM Sodium hydrogen orthophosphate, 2mM EDTA, 5 % w w^{-1} glycerol and 5mM DTT. Lysis buffer with added NaCl (0 – 0.5 M NaCl) was used as running buffer for size exclusion experiments and polishing.

SDS gel electrophoresis used 12 % w v^{-1} self-casted acrylamide gels (per 10 ml: 2ml MQW, 4ml 30 % w v^{-1} acrylamid/bis solution, 3.8 ml 1 M Tris pH 8.8, 0.1 ml 10 % w w^{-1} SDS, 0.1 ml 10 % w w^{-1} ammonium persulphate, 0.04 ml TEMED (all except Tris from BIO RAD Laboratories, USA) with a 4% w v^{-1} stacking layer (per 2 ml: 1.4 ml MQW, 0.33 ml 30 % w v^{-1} acrylamid/bis solution, 0.25 ml 1 M Tris pH 6.8, 0.02 ml 10 % w w^{-1} SDS, 0.02 ml 10 % w w^{-1} ammonium persulphate, 0.002 ml TEMED), using 5X loading buffer composed of 1.9 ml MQW, 0.6 ml 1 M Tris pH 6.8, 5 ml 50 % w w^{-1} glycerol, 10 mg bromphenol blue (BIO RAD Laboratories, USA), 2 ml 10 % w w^{-1} SDS, 0.5 ml beta-mercaptoethanol (BIO RAD Laboratories, USA) and 10X running buffer consisting of 30 g l^{-1} Tris, 144 g l^{-1} glycine (Chem-Supply, Australia), 10 g l^{-1} SDS, pH 8.3. Coomassie Brilliant Blue R-250 staining solution was obtained from BIO RAD Laboratories, USA. A solution of 80 % v v^{-1} MWQ, 10 % v v^{-1} ethanol (Chem-Supply, Australia) and 10 % v v^{-1} acetic acid (Chem-Supply, Australia) was used for destaining.

PEG-6000 was obtained by Chem-Supply, Australia. Lyophilised Unsheared *E.coli* DNA was obtained from Sigma (D4889) and dissolved in MQW.

2.2 Instrumentation

A 5920R centrifuge (Eppendorf, Germany) was used for solid-liquid separation of cell harvest, removal of cell debris and separation of precipitate. Cell disruption was done using a Scientz-IID Ultrasonic homogeniser (Ningbo Scientz Biotechnology, China) with a 6 mm diameter horn. Dynamic light scattering was conducted with a Zetasizer NanoZS (Malvern Panalytical/Spectric, UK). Chromatographic experiments were done using an AKTApure® system equipped with a F9-R fraction collector (GE Healthcare Life Science, Sweden). Superose™ 6 Increase, Capto™ Q and Capto™ MMC columns were obtained from GE Healthcare Life Science, Sweden. Absorbance at 595 nm for Bradford protein assay was measured on an ELx808 microplate absorbance reader (BioTek Instruments, US), UV spectrophotometry for DNA quantification was done on a 2300 Victor X5 multilabel reader (PerkinElmer, US). SDS Gels were run in a Mini-PROTEAN tetra cell (BIO RAD Laboratories, USA).

2.3 Plasmid construction, transformation and host strain

The plasmid was constructed by the Protein Expression Facility of the University of Queensland. Group A Streptococcus antigen GCN4-J8 was inserted into Murine polyomavirus VP1 sequence (M34958) with flanking G4S linkers. The obtained gene VP1 GCN4 J8 was cloned into pETDuet-1 at multiple cloning site 2 (MCS2) at Ndel and Pacl restriction site. The complete sequence was

MAPKRKSGVSKCETKCTKACPRPAPVPKLLIKGGMEVLDLVTGPDSVTEIEAFLNPRMGQP
PTPESLTEGGQYYGWSRGINLATSDTEDSPGNNTLPTWSMAKLQLPMLNEDLTCDTLQM
WEAVSVKTEVVGSGSLLDVHGFNKPTDTVNTKGISTPVEGSQYHVFAVGGEPLDLQGLVT
DARTKYKEEGVVTIKTITKKDMVNKDQVLNPISKAKLDKDGMYPVEIWHPDPAKNENTRYFG
NYTGGTTTPPVLQFTNTLTTVLLDENGVGPLCKGEGLYLSCVDIMGWRVTRGGGGSSQAE
DKVKQSREAKKQVEKALKQLEDKVQAGGGGSYDVHHWRGLPRYFKITLRKRWVKNPYPM
ASLISSLFNNMLPQVQGQPMEGENTQVEEVRVYDGTEPVPGDPDMTRYVDRFGKTKTVFP

220 *GN** which was inserted in the plasmid as following: pT7-lacOp-pT7-lacOp-VP1 – G4S linker
221 – GCN4 J8 – G4S linker.

222 The sequence was verified using Abi BigDye Terminator 3.1. Sequencing, which was
223 conducted by the Australian Genome Research Facility (AGRF).

224 VP1-J8 was transformed into Rosetta™ 2(DE3) Singles™ competent cells (Merck KGaA,
225 Germany) via heat shock transformation using standard procedure. Plasmid DNA was mixed
226 with the competent cells, incubated on ice for 5 min, heat shocked for 30 secs at 42 °C,
227 followed by 2 min cooling on ice. Cells were then mixed with TOC medium and selected on
228 agar plates containing 100 µg ml^{-1} ampicillin and 35 µg ml^{-1} chloramphenicol. A single colony
229 was picked, grown on 50ml TB medium in a 250 ml shake flask at 37 °C. After an optical
230 density OD_{600} of 0.5 AU was reached the cell suspension was mixed with glycerol to a total
231 concentration of 25 % w w^{-1} and stored in 100µl aliquots at -80 °C till further use.

232 *2.4 Protein Expression*

233 One 100 µl aliquot of transferred cells was thawed and poured into 50 ml of TB medium
234 containing antibiotics, in a 250 ml shake flask, and grown overnight at 37 °C at 200 rpm.
235 Next morning 5 ml of the overnight culture was transferred into 200 ml fresh TB medium in a
236 1 l shake flask and grown at 37 °C and 200 rpm. After the optical density OD_{600} reached 0.5
237 AU product expression was started by adding IPTG to a final concentration of 0.1 mmol l^{-1}
238 and lowering the temperature to 27 °C. Product expression lasted 16h, after which cells
239 were harvested by centrifugation at 3200g for 10 min at 4 °C. The pellet was resuspended in
240 0.9 % w w^{-1} saline and divided into 50 ml aliquots and centrifuged for 10 min at 20130 g at 4
241 °C to obtain 1 g pellets. The supernatant was withdrawn and the pellets where then stored at
242 -80 °C until further use.

243 *2.5 Purification of VP1-J8 protein*

244 A 1 g pellet of *E. coli* was resuspended in 50 ml lysis buffer and sonicated for 15 min on ice,
245 using 10 seconds bursts at 400 W followed by 40 seconds cool down phase. After

sonication, the sample was centrifuged at 20130 g for 30 min at 4 °C to obtain clarified supernatant. The VP1-J8 was then precipitated using 3.5 g (7 % w w^{-1}) PEG 6000 and 1.45 g NaCl (0.5 M final concentration). Suspension was gently mixed until the PEG and NaCl were dissolved and incubated on ice for 10 min to form precipitates. After centrifugation at 20130 g at 4 °C for 2 min, the supernatant was discharged and the pellet was gently washed 3 times with 5 ml MQW to remove all residual supernatant. The pellet was then resuspended in 20 ml running buffer containing 0.4 M NaCl. The solution was further purified by an anion exchange step (Capto™ Q) in flow through mode using a running buffer with 0.4 M NaCl at pH 8. A final polishing was achieved using size exclusion chromatography loading 0.5 ml sample on a Superose™ 6 increase column, collecting the peak eluting at 15 ml. If not stated otherwise, running buffer containing 0.4 M NaCl at pH 8 was used with a flowrate of 0.6 ml min^{-1}. Desalting was conducted using a 5 ml HiTrap™ Desalting column (GE Healtcare, Sweden). All buffers and samples were cooled on ice throughout the whole process. The starting material used in the in following described experiments, are summarized in table 1. SDS-PAGE analysis of the different purification steps are provided in the supplementary data.

2.6 Cation exchange experiments on Capto™ MMC

Capto™ MMC was chosen as a cation exchanger as it provides, in contrast to Capto™ S, high binding over a broad range of salt concentrations. Elution is therefore usually done by pH shift. Samples were pre-purified by PEG precipitation as described, and the pellet after precipitation was dissolved in lysis buffer containing 0 M NaCl, at a protein concentration of 1.96 mg ml^{-1}. NaCl was added to a final concentration of 0.5 M NaCl to half of the sample. Lysis buffer containing either 0 M NaCl or 0.5 M NaCl was used as a running buffer and for equilibration. Sample was injected into a 2 ml sample loop and loaded to a 1 ml Capto™ MMC prepacked column at a flow rate of 0.33 ml min^{-1}. The elution was conducted using a 1 M NaCl sodium hydrogen orthophosphate buffer adjusted with NaOH to pH 12. Recovery was estimated by integrating the chromatograms at an absorbance of 280 nm and

comparing peak areas of the flow through during loading and of elution peaks containing VP1-J8.

2.7 Anion exchanger experiments on Capto™ Q

Sample pellets pre-purified by PEG precipitation as described were re-dissolved in lysis buffer at pH 8 either with 0.1 M NaCl or 0.4 M NaCl. Final protein concentration was adjusted to 0.54 mg ml^{-1}. Sample was used to fill a 100 µl sample loop. The pre packed 1 ml Capto™ Q column was equilibrated with the corresponding buffer and loaded at 0.33 ml min^{-1}, followed by a 1 M NaCl step elution, pH 8, at a flow rate of 1 ml min^{-1}.

2.8 Assembling of Virus-like Particles

Purified VP1-J8 capsomeres as described were assembled into virus-like-particles by dialysis against assembling buffer for 24h at 4 °C as described previously (Middelberg et al., 2011). Capsomeres purified by multi modal cation exchange chromatography (Capto™ MMC) followed by SEC chromatography instead of anion exchange chromatography were also assembled into VLP's. The influence of DNA on assembly was examined by preparing VP1-J8 solutions with and without DNA prior to assembly. Host cell DNA free VP1-J8 obtained by AEX and SEC as described in section 2.5 was desalted into lysis buffer pH 8 with 0.1 M NaCl or with 0.5 M NaCl and the concentration of VP1-J8 was adjusted to 0.2 mg ml^{-1}. DNA stock solution to a final concentration of 5 µg ml^{-1} was added to half of the sample. Obtained VLP's were examined by TEM.

2.9 Protein analysis and SDS-PAGE

Protein concentration was measured using the Bradford Protein Assay (Bradford, 1976), following the standard protocol provided by BioRad in 200 µl 96 well plates, with bovine serum albumin as a standard. BSA standard was prepared at different concentrations (0.05 mg ml^{-1}, 0.1 mg ml^{-1}, 0.2 mg ml^{-1} 0.4 mg ml^{-1}) and the concentration was verified measuring the A_{280} absorbance on a NanoDrop. All samples were measured in triplicates.

Self-casted gels as described were used for analysis. If not stated otherwise, 10 µl of sample was mixed with 2 µl of 5X loading buffer and heated at 100 °C for 10 min before loading. A running buffer was used as described with a 200 V fixed current for the entire run. The gel was stained for 1 hour with shaking, followed by 4 h destaining using an ethanol/acetic acid destaining buffer as described. Pictures were obtained on a ChemicDoc imaging system using standard configuration for Comassie Blue gels. Under reducing and denaturing conditions VP1-J8 is expected to be visible at a size of 46.4 kDa.

2.10 DNA Analysis

DNA quantification was conducted using Quant-iT™ High-Sensitivity dsDNA Assay Kit in a 96 well plate, following the manual. Fluorescence was measured at 485/530 nm and all samples were measured in duplicate. Preliminary tests showed that VP1-DNA interactions and aggregates had no influence on the result of the assay.

2.11 Size-exclusion chromatography of VP1-J8 clarified supernatant at different NaCl concentrations by Superose™ 6 Increase

SEC experiments were conducted to measure the elution volume of VP1-J8 capsomeres in crude clarified supernatant at different NaCl concentrations. The larger the molecule, the faster it elutes, therefore aggregates of VP1-J8 capsomeres can be measured in the supernatant. Crude clarified supernatant after cell disruption was obtained as described. The supernatant was split into 6 ml samples and NaCl was added to obtain final concentrations of 0 M, 0.1 M, 0.2 M, 0.3 M, 0.4 M and 0.5 M. After gentle shaking until the salt was dissolved, the samples were stored on ice. A Superose™ 6 Increase 10/300 GL column was equilibrated for 2 column volumes with running buffer having the same NaCl concentration as the sample being examined. Samples were filtered (0.22 µm) and loaded into a 0.5 ml sample loop. Flow rate was 0.6 ml/min, samples were taken every 0.5 ml using the autosampler. Samples (10 µl) were then used for SDS-PAGE analysis.

2.12 Dynamic Light Scattering of VP1-J8 capsomeres and VP1-J8-DNA complexes

To test whether the aggregation of VP1-J8 capsomeres was due to salt-induced precipitation or because of an affinity towards DNA, the hydrodynamic particle size of purified VP1-J8 was measured using dynamic light scattering as this technique allows determination of the hydrodynamic particle diameter at various controlled buffer compositions and is in particular sensitive towards aggregates. SEC could not be easily used because purified VP1-J8 capsomeres did bind to Superose^{TM} 6 Increase and TSKgel® 3000/4000 size exclusion columns at low salt concentrations.

To assess the influences of DNA and NaCl on aggregation, VP1 capsomeres were purified as described. Running buffer for SEC polishing had a NaCl concentration of 0.5 M. The protein concentration of the purified sample was adjusted to 0.01 mg ml^{-1} and no residual DNA could be measured in the sample. The size distribution was measured using dynamic light scattering after which the sample was desalted into 0.1 M NaCl buffer. After desalting the DNA concentration increased to 0.09 ng µl^{-1} which might be residual DNA in the desalting column, contaminating the sample, or may not be a significant measurement noting the assay sensitivity is 0.2 ng µl^{-1}.The desalted sample was measured and to 1 ml of sample 100 µl of unsheared *E. coli* DNA solution (concentration 180 ng / µl) was added. After measurement of the light scattering NaCl was added to a final concentration of 1 M and the sample was incubated for 10 min before a subsequent measurements. As a reference, 100 µl of unsheared *E. coli* DNA solution in 1 ml of MQW was measured.

Samples were stored on ice until measurement. 1 ml of sample was equilibrated for 5 min to 20 °C before starting the measurement. Each reported measurement is an average of 100 individual measurements. Analysis was done using the Zetasizer software by Malvern Technologies.

2.13 Transmission Electron Microscope (TEM) analysis

Samples measured via dynamic light scattering were also examined in a transmission electron microscope. Carbon coated square meshed grids (ProSciTec, standard A) were

plasma cleaned for 15 s right before sample application. 5 µl sample, diluted 1:10 with the corresponding buffer, was pipetted on the mesh and incubated for 5 min. After gently removing excess liquid with a tissue, the grid was washed twice with a drop of MQW to reduce salt crystals. The sample was subsequently stained for 2 min by negative staining using 2 % w v^{-1} uranyl acetate. TEM images were taken on a FEI Tecnai G2 Spirit equipped with an Olympus-SIS Veleta CCD camera at 120kV voltage.

3. Results

3.1 Molecular size distribution of VP1-J8 capsomeres in clarified supernatant at different salt concentrations using size exclusion chromatography

Purified VP1 capsomeres elute at a volume of 15 ml on a Superose™ 6 Increase 10/300 GL column (Ladd Effio, Baumann et al., 2016). VP1-J8 capsomeres have a similar size to VP1 capsomeres (232 kDa versus 212.3 kDa) and are therefore expected to elute at approximately the same volume. Comparing the elution profile of clarified supernatant at different salt concentrations (Fig. 1) no dedicated peak at 15 ml elution volume could be observed at salt concentrations of less than 0.3 M NaCl. However, using a salt concentration of 0.4 M NaCl a peak at 15 ml appeared, which was confirmed to be VP1-J8 by SDS PAGE (Fig. 2).

To measure the size distribution of VP1-J8 capsomeres and to verify the formation of aggregates, samples at different elution volumes from Superose™ 6 Increase were analysed by SDS PAGE (Fig. 2). At salt concentrations lower than 0.3 M NaCl, the majority of VP1-J8 capsomeres were eluted at 9ml (Fig. 2a, 0 M NaCl), at 11ml and 12ml (Fig. 2b, 0.1 M NaCl, and Fig. 2c, 0.2 M NaCl), at 11ml, 12ml and 14ml (Fig. 2d, 0.3 M NaCl). This result indicates the formation of VP1 complexes of several MDa size. In contrast, at salt concentrations above 0.3M NaCl, capsomeres elute at the expected retention volume of ca. 15 ml (Figs. 2e and 2f), indicating no or only minor extents of VP1 complexation.

375 *3.2 Particle size distribution of purified VP1-J8 capsomeres and VP1-J8-DNA complexes*
376 *measured by dynamic light scattering (DLS)*

377 Particle size distributions obtained by dynamic light scattering are shown in Figures 3 and 4.
378 The particle size of purified VP1-J8 capsomeres in 0.5 M NaCl and 0.1 M NaCl buffer is
379 nearly the same, at ca. 10 nm. At 0.1 M NaCl, a small amount of particles (<5 %) show a
380 diameter of 20 nm. This is believed to be due to residual DNA in the desalting column that
381 contaminated the sample, as verified by DNA content after desalting increasing from zero to
382 0.09 ng μl^{-1}. By adding unsheared DNA to VP1-J8 capsomeres, the signal changed
383 drastically and particle diameters larger than 70 nm up to 1000 nm were measured.
384 Unsheared *E. coli* DNA solution at 0 M NaCl, measured as a reference, showed a signal at
385 around 20 nm diameter. The effect could also be reversed as shown in Figure 4. By adding
386 sodium chloride to a final concentration of 1 M NaCl the aggregates broke up and the
387 measured particle size of VP1-J8 plus DNA changed from > 90 nm to < 20 nm.

388 *3.3 TEM analysis of purified VP1-J8 capsomeres and VP1-J8-DNA complexes*

389 Samples measured by DLS were also examined by TEM to confirm the DLS results. Purified
390 VP1-J8 capsomeres are stable in 0.1 M NaCl and do not form aggregates (Figure 5a). After
391 the addition of unsheared *E. coli* DNA irregular aggregates of different sizes are formed, as
392 can been seen in Figure 5b. After subsequent addition of NaCl to a final concentration of 1
393 M, no aggregates could be observed, however very few spherical particles of 40-50 nm
394 diameter could be seen (Fig. 5c).

395 *3.4 Multimodal cation exchange chromatography on Capto™ MMC*

396 Figure 6a shows the absorbance signal of the flow-through during loading. It can be seen,
397 that loading resolubilized VP1-J8 (after PEG precipitation) in a lysis buffer containing 0.5 M
398 NaCl leads to a significantly lower flow through signal (P1), indicating more VP1-J8 is
399 binding on the column, compared to loading at 0 M NaCl (P2). The peak area of the flow
400 through peak decreased from 5366.4 mAu s^{-1} when loaded at 0 M NaCl (P2) to 4791.7 mAu

401 s^{-1} when loaded at 0.5 M NaCl (P1). The elution profile in Figure 6b shows two small elution
402 peaks (P3.1 & P3.2), when loading was at 0 M NaCl, and only one large peak (P4), when
403 loading was done at 0.5 M NaCl. Analysing the peak areas of the elution peaks containing
404 VP1-J8 showed a peak area of 527.8 mAu s^{-1} if loaded at 0.5 M NaCl (P4) and only 52.6
405 mAu s^{-1} if loaded at 0 M NaCl (P3.2). The elution peak area of 527.8 mAu s^{-1} approximates
406 the difference in absorbance signals during loading (574.7 mAu s^{-1}) reasonably well,
407 indicating, that the loaded material eluted completely at the chosen conditions and no
408 material was permanently bound to the column. Therefore, it can be concluded that the
409 binding on Capto™ MMC strongly increased and the recovery increased about 10 times.

410 The SDS-PAGE analysis of the process (Fig. 7) revealed, that if loading was done at 0 M
411 NaCl the majority of VP1-J8 did not bind to the column and remained in the flow through. In
412 contrast, if loading was done at 0.5 M NaCl the majority of VP1-J8 did bind to the column.
413 The first elution peak (P3.1), if loaded at 0 M NaCl, contained only trace amounts of protein,
414 but did also contain DNA. Measured DNA concentration was 3 ng μl^{-1}. The second peak
415 (P3.2) did contain some VP1-J8 at low concentrations and had a DNA content of 0.34 ng μl^{-1}.
416 On the other hand, the whole elution peak after loading at 0.5 M NaCl (P4) did contain
417 high amounts of VP1-J8 and low levels of DNA (0.46 ng μl^{-1}). The DNA concentration of the
418 pre-purified sample was 110.6 ng μl^{-1}.

419 *3.5 Anion exchange chromatography on Capto™ Q*

420 Figures 8a and 8b show chromatograms obtained for loading Capto™ Q at 0.1 M NaCl and
421 0.5 M NaCl, respectively. At low salt concentrations VP1-J8 binds to Capto™ Q, however the
422 capacity is extremely low (<0.2 mg ml^{-1}_{resin} at 2 min column residence time, data not shown).
423 High overloading of the column does not result in significant increase of bound VP1-J8.
424 Interestingly, elution experiments with a linear gradient reveal that the majority of VP1-J8
425 was eluted at the same salt concentration as it lost its affinity towards DNA (ca. 0.3 M NaCl)
426 (chromatogram in supplementary data). If the loading was conducted at salt concentrations
427 above 0.3 M NaCl, VP1-J8 remains in the flow through and DNA can be efficiently removed

as it remains bound to the matrix. The DNA content of the pre-purified sample was 75 ng μl^{-1} and after flow through purification at 0.5 M NaCl loading condition, the DNA content was below the sensitivity of the DNA assay, with a measured value of 0.017 ng μl^{-1}. A comparison of the binding behaviour on the two chromatographic matrixes is summarized in table 2.

3.6 Assembling of virus-like-particles

Both capsomeres obtained by anion exchanger and by multi modal cation exchanger could be assembled into virus-like-particles (determined by TEM, data not shown). Therefore, it can be assumed that the purification pathways do not alter protein integrity.

To test the influence of the presence of DNA on the assembling host cell DNA free VP1-J8 got spiked with DNA as described in section 2.8 to obtain four samples (VP1-J8 with and without DNA in lysis buffer pH 8, at low and at high salt concentrations) were dialysed against assembling buffer. TEM results are shown in figure 9.

At initial NaCl concentrations of 0.5 M NaCl both samples without (figure 9a) or with DNA (figure 9b) assembled predominately into uniform capsid like structures around 45 nm in diameter. Also some smaller particles formed. The capsid like structures assembled without DNA showed a stronger internal staining compared to the one with DNA.
At low initial NaCl concentrations the protein-DNA complexes could not be assembled into capsid like structures (figure 9c). Instead worm like structures of different sizes formed as well as small spherical particles < 20 nm. On the other hand, if no DNA was present at low NaCl concentrations (figure 9d), capsid like structures formed as well as smaller spherical particles of different size. Compared to the samples with higher initial NaCl, the samples with lower NaCl concentrations were less uniform.

4. Discussion

One of the major issues of purifying viral capsomeres and viral structures, either as a wild type or presenting a foreign antigen, is the poor binding onto chromatographic media and

hence low recovery yields. That VP1 capsomeres in crude lysate form soluble aggregates of different size, is an observation that has already been made (Lipin et al., 2008). Different mechanisms have been suggested, for example polymerization because of the used GST tag or aggregation because of inserted hydrophobic antigens (Abidin et al., 2015; Lipin et al., 2008). These size exclusion experiments on GST-free non-purified proteins show that non purified VP1-J8 forms aggregates below a NaCl concentration of 0.3 M. This can have various reasons, like salt dependent solubility, intermolecular attractions or the interaction with other molecules such as DNA. Polymerization because of affinity tags however, can be excluded as no affinity tag is used in these experiments.

Light scattering experiments of purified VP1-J8 revealed that purified VP1-J8 capsomeres are indeed stable at low salt concentrations and aggregates are formed due to an interaction with DNA. It could also be shown that this is a reversible interaction, as the aggregates disassociate if the salt concentration is raised, indicating that the DNA VP1-J8 interaction is a non-specific electrostatic interaction. The slight increase of the measured hydrodynamic size of dissociated capsomeres compared to the starting material before the addition of DNA might be a result of overlapping signals of DNA and capsomeres, as dynamic light scattering is not capable of resolving multiple narrow species. However, as this technique is in particular sensitive towards larger particles it can be assumed no aggregates were present. The results were verified by TEM showing no aggregated VP1-J8 at low salt concentrations in the absence of DNA, and irregular shaped aggregates after the addition of DNA and the formed aggregates could be dissociated by applying a high salt concentration. Why some large, capsid-like aggregates could be observed at the TEM of capsomeres in high salt (Figure 5c) can only be speculated as there was no calcium in the solution, which is considered to be mandatory for self-assembling of VP1 capsomeres into well-formed virus-like-particles (Chuan et al., 2010; Schmidt, Rudolph, & Bohm, 2000). Maybe an increase of the hydrophobic attraction due to the high salt concentration and depleted DTT due to long exposure during processing, lead to a degree of capsomeres self-assembly, an effect that

has also been observed in the past (Salunke, Caspar, & Garcea, 1986). This process might be also mediated by “right sized” DNA fragments in the solution, supporting assembly, as a similar mechanism was proposed (Ou et al., 1999; van Rosmalen, Li, Zlotnick, Wuite, & Roos, 2018).

To measure the influence of these aggregates on chromatographic purification, experiments with cation and anion exchangers were conducted. The assumption was that, in an aggregated form, the capsomeres cannot access the pores of chromatographic resin which typically have a diameter of roughly 40-80 nm, and therefore can only bind to the outer surface, leading to very low binding capacitates (J. Avallin et al., 2016). This assumption was proven as only minor amounts of VP1-J8 bound on multimodal cation exchanger columns (Capto™ MMC) when loaded at low salt concentrations. A pure cation exchanger like Capto™ S showed comparable low binding capacities at low salt concentrations (data not shown). Using a salt-tolerant cation exchanger (Capto™ MMC), which keeps a high binding capacity over a broad range of salt concentrations, it could be shown that the binding increased dramatically, and the majority of VP1-J8 protein was captured, if a salt concentration above the dissociation concentration was used. The enhanced binding leads to an increased recovery during the chromatographic purification.. This can be explained by the fact that now non-aggregated capsomeres, having a size of 10-15 nm, could access the pores in the resin.

Another phenomenon was observed, namely that at low salt concentrations not only the capsomeres bound to a cation exchanger column, but also DNA. As DNA usually does not bind to a cation exchanger at pH 8, it likely bound to the capsomeres that were captured on the column, suggesting again the existence of DNA-protein complexes.

A purification method for viral capsomeres and viral capsids, proposed in the literature, is the use of strong anion-exchange membrane columns in bind and elute mode (Ladd Effio, Baumann et al., 2016). Interestingly the capsomeres do bind to Capto Q resins, a strong anion exchanger, at the same pH value (pH 8) as they do bind to cation exchangers

(Capto™ S, POROS™ HS and Capto™ MMC). These experiments show that at low salt concentrations VP1-J8 binds to the column, however the capacity is extremely low, which again can be explained by poor accessibility to matrix pores, because of formed DNA-protein aggregates. The formation of aggregates also explains the comparably high reported capacities on membrane columns (Ladd Effio, Hahn et al., 2016). Another interesting fact is that the capsomeres elute from anion exchangers at the same salt concentration as the DNA-protein aggregates dissociate, opening the question of the binding mechanism. Instead of actually binding onto the column proper, the VP1 capsomeres might actually bind to DNA, which then binds to the anion exchanger in a layer-by-layer process. This might be an explanation for the strange binding isotherms described for Sf9 insect cell-derived virus-like-particles, as the binding capacity would be dependent on the protein-DNA ratio (Ladd Effio, Hahn et al., 2016).

Some DNA interactions with VP1 capsomere have been previously described. Early research found that VP1 capsomeres show a high affinity towards DNA, that this affinity is not sequence specific, and that VP1 capsomeres do elute from a DNA-cellulose column at salt concentrations between 0.3 and 0.4 M NaCl (Chang et al., 1993; Moreland et al., 1991). This is congruent with the observation that DNA-VP1-J8 complexes dissociate at NaCl concentrations above 0.3 M and also explains that the DNA-protein complexes can form with bacterial DNA or DNA of other sources. DNA-protein complex formation was also found by Štokrová et al. (1999) who showed that VP1 capsomeres coat circular DNA, as expected for viral packaging of nucleic acids in the native virus.

Another point is that the disassembly of polyomavirus results not only in free capsomeres but also in DNA-capsomere complexes (Brady JN, Winston VD, & Consigli RA., 1978). The reason why only some of the capsomeres form complexes, if viral capsids are dissembled, might be due the ratio of DNA to capsomeres, as there may have been insufficient DNA for all capsomeres to bind to.

The influence of DNA-capsomere interactions on production, stability, assembling and purification of VP1 capsomeres has, however, been significantly underestimated. Especially if these capsomeres are produced in bacterial systems in an environment with excess DNA. Under such conditions it is highly likely that the majority of VP1 is bound to host-cell DNA, therefore forming large aggregates.

Assembling of capsomere-DNA complexes into VLPs was not possible in our experiments. Instead worm like aggregates of different sizes formed. These worm like aggregates do not form if the salt concentration is above the protein-DNA dissociation concentration and instead virus-like particle form, comparable to the assembly without DNA. The type and length of the present nucleic acid might play an important role on the shape and size of these aggregates (Ruiter et al., 2019) and comparable tubular aggregates can be found in the nucleus of infected cells (Erickson et al., 2012). Protein-DNA interactions therefore can be an explanation for at least some types of aggregates formed during assembly.
A recent study proposed that DNA can influence the assembly process beneficially, as less wrong size particles are formed (van Rosmalen et al., 2018). This phenomenon however, could not be observed in our experiments as assembly products at high salt concentration, with or without DNA, showed well defined capsid like structures. Nevertheless, the presence of DNA seems to influence the assembly process and therefore the DNA-protein interaction needs to be tightly controlled to obtain reliable results. However, this topic still needs further investigation to understand the underlying mechanism.

Knowing that VP1 forms complexes with DNA at low salt concentrations, a few conclusions for purification can be made. At low salt concentrations VP1 or VP1 based vaccine candidates will bind onto conventional chromatographic media at low efficiency, as the complexes cannot enter the pores of the resin. An alternative is the use of membrane columns, monoliths or resins with large pores like POROS™ as shown in the literature (Ladd Effio, Baumann et al., 2016). Another and preferable option is the use of conventional salt tolerant media like Capto™ MMC together with buffers having a salt concentration above the

561 DNA-capsomere dissociation concentration, as they are widely available, cheap and easy to
562 scale. This approach leads to highly efficient binding and eradicates one of the main
563 bottlenecks during purification.

564 DNA can only be efficiently removed if a salt concentration above the dissociation
565 concentration is used during the process, as otherwise DNA and capsomeres will co-elute.
566 Until complete removal of DNA, the capsomeres will be not stable in low salt concentration
567 buffers. This is particularly important for alternative purification strategies like precipitation
568 and extraction in which DNA is usually incompletely removed. The binding on anion
569 exchangers might be mediated by DNA and therefore the ratio of DNA to VP1 in the lysate
570 will affect the binding capacity and overall process behaviour. It is furthermore not possible
571 to assemble DNA-VP1 complexes into virus-like particles. Above the dissociating salt
572 concentration however, the presence of DNA seems not to affect the assembly negatively.

573 **5. Conclusion**

574 Murine polyomavirus major capsid protein VP1 forms DNA-protein complexes of different
575 sizes in buffers having low salt concentrations. It was shown that these aggregates have a
576 significant impact on the bioprocessing of VP1 pentamers, as it was not possible to
577 assemble these complexes into VLPs. Instead of spherical particles, tubular aggregates
578 formed. Furthermore, the DNA-protein complexes lead to poor chromatographic recovery
579 due to low pore accessibility. By increasing the salt concentration of the buffer above 0.3 M
580 NaCl (pH 8) the DNA-protein complexes dissociate and uniform VLPs can be assembled
581 even in the presence of DNA. The approach of processing VP1 in buffers having a NaCl
582 concentration above the protein-DNA dissociation concentration dramatically improved the
583 chromatographic binding behaviour and the binding capacity increased by at least an order
584 of magnitude. Those findings lead to the development of efficient purification strategies of
585 VP1-J8, using salt tolerant multi modal cation exchanger, removing most of the host cell
586 DNA and protein without significant product loss. Since DNA affinity is an inherent property

of viral proteins, similar approaches are likely applicable for other viral proteins and will help to develop efficient bioprocessing strategies for viral proteins.

Acknowledgements

The authors declare that there is no conflict of interest.

Author contribution

Lukas Gerstweiler conceived the original research idea, designed and performed the study, wrote the manuscript and carried out experimental work. Jingxiu Bi supervised the project and assisted with conceptualization and writing. Anton Middelberg supervised the project and contributed to conceptualization, experimental design and analysis, and writing.

All authors reviewed and approved the manuscript

References

Abidin, R. S., Lua, L. H. L. [L. H. L.], Middelberg, A. P. J. [A. P. J.], & Sainsbury, F. [F.] (2015). Insert engineering and solubility screening improves recovery of virus-like particle subunits displaying hydrophobic epitopes. *Protein Science : A Publication of the Protein Society*, *24*(11), 1820–1828. https://doi.org/10.1002/pro.2775

Al-Barwani, F., Donaldson, B., Pelham, S. J., Young, S. L., & Ward, V. K. (2014). Antigen delivery by virus-like particles for immunotherapeutic vaccination. *Therapeutic Delivery*, *5*(11), 1223–1240. https://doi.org/10.4155/tde.14.74

Anggraeni, M. R., Connors, N. K., Wu, Y., Chuan, Y. P. [Yap P.], Lua, L. H. L., & Middelberg, A. P. J. (2013). Sensitivity of immune response quality to influenza helix 190 antigen structure displayed on a modular virus-like particle. *Vaccine*, *31*(40), 4428–4435. https://doi.org/10.1016/j.vaccine.2013.06.087

Bradford, M. M. (1976). A rapid and sensitive method for the quantitation of microgram quantities of protein utilizing the principle of protein-dye binding. *Analytical Biochemistry*, *72*(1-2), 248–254. https://doi.org/10.1016/0003-2697(76)90527-3

Brady JN, Winston VD, & Consigli RA. (1978). Characterization of a DNA-protein complex and capsomere subunits derived from polyoma virus by treatment with ethyleneglycol-bis-N,N'-tetraacetic acid and dithiothreitol. *Journal of Virology*, 193–204.

Bright, R. A., Carter, D. M., Daniluk, S., Toapanta, F. R., Ahmad, A., Gavrilov, V., . . . Ross, T. M. (2007). Influenza virus-like particles elicit broader immune responses than whole virion inactivated influenza virus or recombinant hemagglutinin. *Vaccine*, *25*(19), 3871–3878. https://doi.org/10.1016/j.vaccine.2007.01.106

Buch, M. H. C., Liaci, A. M., O'Hara, S. D., Garcea, R. L. [Robert L.], Neu, U., & Stehle, T. (2015). Structural and Functional Analysis of Murine Polyomavirus Capsid Proteins Establish the Determinants of Ligand Recognition and Pathogenicity. *PLoS Pathogens*, *11*(10), e1005104. https://doi.org/10.1371/journal.ppat.1005104

Carapetis, J. R., Steer, A. C., Mulholland, E. K., & Weber, M. (2005). The global burden of group A streptococcal diseases. *The Lancet Infectious Diseases*, *5*(11), 685–694. https://doi.org/10.1016/S1473-3099(05)70267-X

Carter, Donald M.; Darby, Christopher A.; Lefoley, Bradford C.; Crevar, Corey J.; Alefantis, Timothy; Oomen, Raymond et al. (2016): Design and Characterization of a Computationally Optimized Broadly Reactive Hemagglutinin Vaccine for H1N1 Influenza Viruses. In Journal of Virology 90 (9), pp. 4720–4734. https://doi.org/10.1128/JVI.03152-15.

Cavelti-Weder, C., Timper, K., Seelig, E., Keller, C., Osranek, M., Lässing, U., . . . Bachmann, M. F. (2016). Development of an Interleukin-1β Vaccine in Patients with Type 2 Diabetes. *Molecular Therapy : The Journal of the American Society of Gene Therapy*, *24*(5), 1003–1012. https://doi.org/10.1038/mt.2015.227

659 Chang, D., Cai, X., & Consigli, R. A. (1993). Characterization of the DNA binding properties
660 of polyomavirus capsid proteins. *Journal of Virology*, *67*(10), 6327–6331.
661 Chuan, Y. P. [Yap P.], Fan, Y. Y., Lua, L. H. L., & Middelberg, A. P. J. (2010). Virus
662 assembly occurs following a pH- or Ca2+-triggered switch in the thermodynamic
663 attraction between structural protein capsomeres. *Journal of the Royal Society, Interface*,
664 *7*(44), 409–421. https://doi.org/10.1098/rsif.2009.0175
665 Chuan, Y. P. [Yap P.], Wibowo, N., Lua, L. H.L. [Linda H.L.], & Middelberg, A. P.J. (2014).
666 The economics of virus-like particle and capsomere vaccines. *Biochemical Engineering*
667 *Journal*, *90*, 255–263. https://doi.org/10.1016/j.bej.2014.06.005
668 Cornuz, J., Zwahlen, S., Jungi, W. F., Osterwalder, J., Klingler, K., van Melle, G., . . .
669 Cerny, T. (2008). A vaccine against nicotine for smoking cessation: A randomized
670 controlled trial. *PloS One*, *3*(6), e2547. https://doi.org/10.1371/journal.pone.0002547
671 Ding, Y., Chuan, Y. P. [Yap Pang], He, L., & Middelberg, A. P. J. (2010). Modeling the
672 competition between aggregation and self-assembly during virus-like particle processing.
673 *Biotechnology and Bioengineering*, *107*(3), 550–560. https://doi.org/10.1002/bit.22821
674 Donaldson, B., Al-Barwani, F., Pelham, S. J., Young, K., Ward, V. K., & Young, S. L. (2017).
675 Multi-target chimaeric VLP as a therapeutic vaccine in a model of colorectal cancer.
676 *Journal for Immunotherapy of Cancer*, *5.* https://doi.org/10.1186/s40425-017-0270-1
677 Donaldson, B., Lateef, Z., Walker, G. F., Young, S. L., & Ward, V. K. (2018). Virus-like
678 particle vaccines: Immunology and formulation for clinical translation. *Expert Review of*
679 *Vaccines*, *17*(9), 833–849. https://doi.org/10.1080/14760584.2018.1516552
680 Effio, C. L., & Hubbuch, J. (2015). Next generation vaccines and vectors: Designing
681 downstream processes for recombinant protein-based virus-like particles. *Biotechnology*
682 *Journal*, *10*(5), 715–727. https://doi.org/10.1002/biot.201400392
683 Erickson, K. D., Bouchet-Marquis, C., Heiser, K., Szomolanyi-Tsuda, E., Mishra, R.,
684 Lamothe, B., . . . Garcea, R. L. [Robert L.] (2012). Virion assembly factories in the
685 nucleus of polyomavirus-infected cells. *PLoS Pathogens*, *8*(4), e1002630.
686 https://doi.org/10.1371/journal.ppat.1002630
687 Frazer, I. H. (2004). Prevention of cervical cancer through papillomavirus vaccination. *Nature*
688 *Reviews. Immunology*, *4*(1), 46–54. https://doi.org/10.1038/nri1260
689 Gillock, E. T., Rottinghaus, S., Chang, D., Cai, X., Smiley, S. A., An, K., & Consigli, R. A.
690 (1997). Polyomavirus major capsid protein VP1 is capable of packaging cellular DNA
691 when expressed in the baculovirus system. *Journal of Virology*, *71*(4), 2857–2865.
692 Guo, J., Zhou, A., Sun, X., Sha, W., Ai, K., Pan, G., . . . He, S. (2019). Immunogenicity of a
693 Virus-Like-Particle Vaccine Containing Multiple Antigenic Epitopes of Toxoplasma gondii
694 Against Acute and Chronic Toxoplasmosis in Mice. *Frontiers in Immunology*, *10*, 592.
695 https://doi.org/10.3389/fimmu.2019.00592
696 Hume, H. K., Vidigal, J., Carrondo, M. J. T., Middelberg, A. P. J., Roldão, A., & Lua, L. H. L.
697 (2019). Synthetic biology for bioengineering virus-like particle vaccines. *Biotechnology*
698 *and Bioengineering*, *116*(4), 919–935. https://doi.org/10.1002/bit.26890
699 J. Avallin, A. Nilsson, M. Asplund, N. Pettersson, T. Searle, & C. Jägersten (2016). *Columns*
700 *Upto 1600 Mm in Diameter Packed with Protein A Chromatography Medium Using Axial*
701 *Mechanical Compression.*
702 Johne, R., & Müller, H. (2004). Nuclear localization of avian polyomavirus structural protein
703 VP1 is a prerequisite for the formation of virus-like particles. *Journal of Virology*, *78*(2),
704 930–937. https://doi.org/10.1128/JVI.78.2.930-937.2004

Ladd Effio, C., Baumann, P., Weigel, C., Vormittag, P., Middelberg, A., & Hubbuch, J. (2016). High-throughput process development of an alternative platform for the production of virus-like particles in Escherichia coli. *Journal of Biotechnology*, *219*, 7–19. https://doi.org/10.1016/j.jbiotec.2015.12.018

Ladd Effio, C., Hahn, T., Seiler, J., Oelmeier, S. A., Asen, I., Silberer, C., . . . Hubbuch, J. (2016). Modeling and simulation of anion-exchange membrane chromatography for purification of Sf9 insect cell-derived virus-like particles. *Journal of Chromatography A.*, *1429*, 142–154. https://doi.org/10.1016/j.chroma.2015.12.006

Li, P. P., Naknanishi, A., Tran, M. A., Ishizu, K.-I., Kawano, M., Phillips, M., . . . Kasamatsu, H. (2003). Importance of Vp1 calcium-binding residues in assembly, cell entry, and nuclear entry of simian virus 40. *Journal of Virology*, *77*(13), 7527–7538. https://doi.org/10.1128/JVI.77.13.7527-7538.2003

Liew, M. W. O., Rajendran, A., & Middelberg, A. P. J. (2010). Microbial production of virus-like particle vaccine protein at gram-per-litre levels. *Journal of Biotechnology*, *150*(2), 224–231. https://doi.org/10.1016/j.jbiotec.2010.08.010.

Lipin, D. I., Lua, L. H. L., & Middelberg, A. P. J. (2008). Quaternary size distribution of soluble aggregates of glutathione-S-transferase-purified viral protein as determined by asymmetrical flow field flow fractionation and dynamic light scattering. *Journal of Chromatography A.*, *1190*(1-2), 204–214. https://doi.org/10.1016/j.chroma.2008.03.032

Lipin, D. I., Raj, A., Lua, L. H. L., & Middelberg, A. P. J. (2009). Affinity purification of viral protein having heterogeneous quaternary structure: Modeling the impact of soluble aggregates on chromatographic performance. *Journal of Chromatography A.*, *1216*(30), 5696–5708. https://doi.org/10.1016/j.chroma.2009.05.082

Lua, L. H. L., Connors, N. K., Sainsbury, F. [Frank], Chuan, Y. P. [Yap P.], Wibowo, N., & Middelberg, A. P. J. (2014). Bioengineering virus-like particles as vaccines. *Biotechnology and Bioengineering*, *111*(3), 425–440. https://doi.org/10.1002/bit.25159

Mobini, Saeed; Chizari, Milad; Mafakher, Ladan; Rismani, Elmira; Rismani, Elham (2020): Computational Design of a Novel VLP-Based Vaccine for Hepatitis B Virus. In Frontiers in Immunology 11, p. 2074. https://doi.org/10.3389/fimmu.2020.02074.

Middelberg, A. P. J., Rivera-Hernandez, T., Wibowo, N., Lua, L. H. L., Fan, Y. [Yuanyuan], Magor, G., . . . Batzloff, M. R. (2011). A microbial platform for rapid and low-cost virus-like particle and capsomere vaccines. *Vaccine*, *29*(41), 7154–7162. https://doi.org/10.1016/j.vaccine.2011.05.075

Mohr, J., Chuan, Y. P. [Yap P.], Wu, Y., Lua, L. H. L., & Middelberg, A. P. J. (2013). Virus-like particle formulation optimization by miniaturized high-throughput screening. *Methods (San Diego, Calif.)*, *60*(3), 248–256. https://doi.org/10.1016/j.ymeth.2013.04.019

Moreland, R.B., Montross, L., & Garcea, R. L. [R. L.] (1991). Characterization of the DNA-binding properties of the polyomavirus capsid protein VP1. *Journal of Virology*, *65*, 1168–1176.

Ou, W. C., Wang, M., Fung, C. Y., Tsai, R. T., Chao, P. C., Hseu, T. H., & Chang, D. (1999). The major capsid protein, VP1, of human JC virus expressed in Escherichia coli is able to self-assemble into a capsid-like particle and deliver exogenous DNA into human kidney cells. *The Journal of General Virology*, *80 (Pt 1)*, 39–46. https://doi.org/10.1099/0022-1317-80-1-39

Pattenden, L. K., Middelberg, A. P. J., Niebert, M., & Lipin, D. I. (2005). Towards the preparative and large-scale precision manufacture of virus-like particles. *Trends in Biotechnology*, *23*(10), 523–529. https://doi.org/10.1016/j.tibtech.2005.07.011

Pattinson, D. J., Apte, S. H., Wibowo, N., Chuan, Y. P. [Yap P.], Rivera-Hernandez, T., Groves, P. L., . . . Doolan, D. L. (2019). Chimeric Murine Polyomavirus Virus-Like Particles Induce Plasmodium Antigen-Specific CD8+ T Cell and Antibody Responses. *Frontiers in Cellular and Infection Microbiology*, *9*, 215. https://doi.org/10.3389/fcimb.2019.00215

Rivera-Hernandez, T., Hartas, J., Wu, Y., Chuan, Y. P. [Yap P.], Lua, L. H. L., Good, M., . . . Middelberg, A. P. J. (2013). Self-adjuvanting modular virus-like particles for mucosal vaccination against group A streptococcus (GAS). *Vaccine*, *31*(15), 1950–1955. https://doi.org/10.1016/j.vaccine.2013.02.013

Ruiter, M. V. de, van der Hee, R. M., Driessen, A. J. M., Keurhorst, E. D., Hamid, M., & Cornelissen, J. J. L. M. (2019). Polymorphic assembly of virus-capsid proteins around DNA and the cellular uptake of the resulting particles. *Journal of Controlled Release : Official Journal of the Controlled Release Society*, *307*, 342–354. https://doi.org/10.1016/j.jconrel.2019.06.019

Salunke, D. M., Caspar, D. L.D., & Garcea, R. L. [Robert L.] (1986). Self-assembly of purified polyomavirus capsid protein VP1. *Cell*, *46*(6), 895–904. https://doi.org/10.1016/0092-8674(86)90071-1

Schmidt, U., Rudolph, R., & Bohm, G. (2000). Mechanism of Assembly of Recombinant Murine Polyomavirus-Like Particles. *Journal of Virology*, *74*(4), 1658–1662. https://doi.org/10.1128/JVI.74.4.1658-1662.2000

Seth, A., Kong, I. G., Lee, S.-H., Yang, J.-Y., Lee, Y.-S., Kim, Y., . . . Kweon, M.-N. (2016). Modular virus-like particles for sublingual vaccination against group A streptococcus. *Vaccine*, *34*(51), 6472–6480. https://doi.org/10.1016/j.vaccine.2016.11.008

Simon, Claudia; Schaepe, Sebastian; Breunig, Karin; Lilie, Hauke (2013): Production of polyomavirus-like particles in a Klgal80 knockout strain of the yeast Kluyveromyces lactis. In Preparative Biochemistry & Biotechnology 43 (2), pp. 217–235. DOI: https://doi.org/10.1080/10826068.2012.750613

Štokrová, J., Palková, Z., Fischer, L., Richterová, Z., Korb, J., Griffin, B. E., & Forstová, J. (1999). Interactions of heterologous DNA with polyomavirus major structural protein, VP1. *FEBS Letters*, *445*(1), 119–125. https://doi.org/10.1016/S0014-5793(99)00003-4

Tekewe, A., Connors, N. K., Middelberg, A. P. J., & Lua, L. H. L. (2016). Design strategies to address the effect of hydrophobic epitope on stability and in vitro assembly of modular virus-like particle. *Protein Science : A Publication of the Protein Society*, *25*(8), 1507–1516. https://doi.org/10.1002/pro.2953

Tekewe, A., Connors, N. K., Sainsbury, F. [Frank], Wibowo, N., Lua, L. H.L. [Linda H.L.], & Middelberg, A. P.J. (2015). A rapid and simple screening method to identify conditions for enhanced stability of modular vaccine candidates. *Biochemical Engineering Journal*, *100*, 50–58. https://doi.org/10.1016/j.bej.2015.04.004

Tekewe, A., Fan, Y. [Yuanyuan], Tan, E., Middelberg, A. P. J., & Lua, L. H. L. (2017). Integrated molecular and bioprocess engineering for bacterially produced immunogenic modular virus-like particle vaccine displaying 18 kDa rotavirus antigen. *Biotechnology and Bioengineering*, *114*(2), 397–406. https://doi.org/10.1002/bit.26068

Teunissen, E. A., Raad, M. de, & Mastrobattista, E. (2013). Production and biomedical applications of virus-like particles derived from polyomaviruses. *Journal of Controlled Release : Official Journal of the Controlled Release Society*, *172*(1), 305–321. https://doi.org/10.1016/j.jconrel.2013.08.026

Van Rosmalen, M. G. M., Li, C., Zlotnick, A., Wuite, G. J. L., & Roos, W. H. (2018). Effect of dsDNA on the Assembly Pathway and Mechanical Strength of SV40 VP1 Virus-like

Particles. *Biophysical Journal*, *115*(9), 1656–1665. https://doi.org/10.1016/j.bpj.2018.07.044

VBI Vaccines Inc (2018). Immunogenicity and Safety of Sci-B-Vac™ to Engerix-B® in Adults ≥ 18 Years Old and Superiority in Adults ≥ 45 Years Old.: ClinicalTrials.gov Identifier: NCT03393754. *National Library of Medicine*. Retrieved from https://clinicaltrials.gov/ct2/show/NCT03393754

Vekemans, J., Gouvea-Reis, F., Kim, J. H., Excler, J.-L., Smeesters, P. R., O'Brien, K. L., . . . Kaslow, D. C. (2019). The Path to Group A Streptococcus Vaccines: World Health Organization Research and Development Technology Roadmap and Preferred Product Characteristics. *Clinical Infectious Diseases : An Official Publication of the Infectious Diseases Society of America*, *69*(5), 877–883. https://doi.org/10.1093/cid/ciy1143

Wibowo, N., Chuan, Y. P. [Yap P.], Lua, L. H.L. [Linda H.L.], & Middelberg, A. P.J. (2013). Modular engineering of a microbially-produced viral capsomere vaccine for influenza. *Chemical Engineering Science*, *103*, 12–20. https://doi.org/10.1016/j.ces.2012.04.001

The World Bank (2018). Summary of Chapter 1: Ending Global Poverty. Retrieved from http://pubdocs.worldbank.org/en/911401537279777945/PSPR2018-Ch1-Summary-EN.pdf

Wu, C.-Y., Yeh, Y.-C., Yang, Y.-C., Chou, C., Liu, M.-T., Wu, H.-S., . . . Hsiao, P.-W. (2010). Mammalian expression of virus-like particles for advanced mimicry of authentic influenza virus. *PloS One*, *5*(3), e9784. https://doi.org/10.1371/journal.pone.0009784

Zaveckas, Mindaugas; Goda, Karolis; Ziogiene, Danguole; Gedvilaite, Alma (2018): Purification of recombinant trichodysplasia spinulosa-associated polyomavirus VP1-derived virus-like particles using chromatographic techniques. In Journal of Chromatography B, Analytical technologies in the biomedical and life sciences 1090, pp. 7–13. https://doi.org/10.1016/j.jchromb.2018.05.007.

Zhai, L., Peabody, J., Pang, Y.-Y. S., Schiller, J., Chackerian, B., & Tumban, E. (2017). A novel candidate HPV vaccine: Ms2 phage VLP displaying a tandem HPV L2 peptide offers similar protection in mice to Gardasil-9. *Antiviral Research*, *147*, 116–123. https://doi.org/10.1016/j.antiviral.2017.09.012

Zhang, L., Lua, L. H. L., Middelberg, A. P. J., Sun, Y., & Connors, N. K. (2015). Biomolecular engineering of virus-like particles aided by computational chemistry methods. *Chemical Society Reviews*, *44*(23), 8608–8618. https://doi.org/10.1039/c5cs00526d

Zhou, X., Bai, H., Kataoka, M., Ito, M., Muramatsu, M., Suzuki, T., & Li, T.-C. (2019). Characterization of the self-assembly of New Jersey polyomavirus VP1 into virus-like particles and the virus seroprevalence in Japan. *Scientific Reports*, *9*(1), 13085. https://doi.org/10.1038/s41598-019-49541-y

Figures – Caption

Table 1: Starting material used for the different experiments.

Table 2. Binding behaviour of resolubilized (after PEG precipitation) VP1-J8 and DNA to a multi modal cation exchanger (Capto™ MMC) and a strong anion exchanger (Capto™ Q) at pH 8. At salt concentrations < 0.3 M NaCl VP1-J8 is binding to DNA and forming complexes.

Figure 1. Size exclusion chromatogram of clarified supernatant containing VP1-J8 capsomeres at different NaCl concentrations of the sample. Running buffer had the same composition as the sample. Vertical line indicates the volume (15 ml) at which the capsomeres are expected to elute. (· · ·) 0.1 M NaCl, (- - -) 0.2 M NaCl, (- · - ·) 0.3 M NaCl, (—) 0.4 M NaCl.

Figure 2. SDS-PAGE analysis of size exclusion fractions of clarified supernatant containing VP1-J8 at different salt concentrations and pH 8. (A) 0 M NaCl, (B) 0.1 M NaCl, (C) 0.2 M NaCl, (D) 0.3 M NaCl, (E) 0.4 M NaCl, (F) 0.5 M NaCl.

Figure 3. Size distribution of VP1-J8 capsomeres with and without DNA measured by dynamic light scattering at different buffer composition. (·····) VP1-J8 in 0.1 M NaCl, (-·-·-) VP1-J8 in 0.5 M NaCl, (- - -) DNA in 0 M NaCl (MQW), (—) VP1-J8 + DNA in 0.1 M NaCl.

Figure 4. Size distribution of VP1-J8 capsomeres containing DNA, measured by dynamic light scattering, in 0.1 M NaCl (—) and after adding NaCl to a final concentration of 1 M NaCl (- - -).

Figure 5. (A) TEM image of purified VP1-J8 capsomeres in 0.1 M NaCl buffer pH 8, containing no DNA. (B) Purified VP1-J8 capsomeres plus unsheared *E.coli* DNA in 0.1 M NaCl buffer pH 8. (C)The same sample as in (B) after the addition of NaCl to a final concentration of 1 M. The scale bar corresponds to 100 nm distance

Figure 6. (A) Column loading. Absorbance at 280 nm obtained from the flowthrough while loading 2 ml of resolubilized VP1-J8 (after PEG precipitation) at NaCl concentrations of 0.5 M (—) or 0 M (- --) at pH = 8 onto a 1 ml multimodal weak cation exchanger (Capto™ MMC), loading started at 0 ml (B) Column eluting. Elution profile after loading resolubilized VP1-J8 (after PEG precipitation) at NaCl concentrations of 0.5 M (—) or 0 M (- - -) at pH = 8 onto a 1 ml multimodal weak cation exchanger (Capto™ MMC). Elution was obtained by applying a step gradient of 1 M NaCl phosphate buffer at pH 12 starting at 13.5 ml. The elution buffer had a different absorbance compared to the binding buffer, caused by the instability of DTT, resulting in a baseline shift towards the end of the chromatogram.

Figure 7. SDS-PAGE analysis of the bind and elute experiments of VP1-J8 onto Capto™ MMC (Figure 6). Lanes (1) & (4) correspond to the starting material used for loading at 0.5 M

NaCl (lane 1) and 0 M NaCl (lane 4). (2) Flow through of loading at 0.5 M NaCl, (3) Elution after loading at 0.5 M NaCl, (5) Flow through of loading at 0 M NaCl, (6) First elution peak after loading at 0 M NaCl, (7) Second elution peak after loading at 0 M NaCl.

Figure 8. (A) Anion exchange chromatography elution of resolubilized VP1-J8 (after PEG precipitation) loaded on a 1 ml CaptoTM Q column at 0.1 M NaCl, pH8. Only a minimal flow through can be observed and most of the protein, including VP1-J8 did bind to the column. VP1-J8 does elute in a first peak at 5ml, followed by a peak of mostly impurities. (—) Absorbance A280, (- - -) Conductivity. (B) Anion exchange chromatography elution of resolubilized VP1-J8 (after PEG precipitation) loaded on a 1 ml CaptoTM Q column at 0.5 M NaCl, pH8. VP1-J8 is not binding to the column and remains in the flow through that elutes at 0.5 ml. (—) Absorbance A280, (- - -) Conductivity.

Figure 9. Assembly products of VP1 with and without DNA at different initial NaCl concentrations. Scale bar represents 100 nm. (A) 0.5 M NaCl no DNA. (B) 0.5 M NaCl plus DNA. (C) 0.1 M NaCl plus DNA. (D) 0.1M NaCl no DNA.

Tables

Table 1: Starting material used for the different experiments.

Experiment	Starting material	Host cell DNA	DNA spiking
2.6 Cation exchange	Resolubilized PEG precipitate	Yes	No
2.7 Anion exchange	Resolubilized PEG precipitate	Yes	No
2.8 Assembly	Purified VP1-J8 (PEG + AEX + SEC)	No	Yes
2.11 SEC	Clarified lysate	Yes	No
2.12 Light Scattering	Purified VP1-J8 (PEG + AEX + SEC)	No	Yes

Table 2. Binding behaviour of resolubilized (after PEG precipitation) VP1-J8 and DNA to a multi modal cation exchanger (Capto™ MMC) and a strong anion exchanger (Capto™ Q) at pH 8.

	Capto™ MMC		Capto™ Q	
loading buffer	VP1-J8 binding	DNA binding	VP1-J8 binding	DNA binding
pH 8 c(NaCl) < 0.3 M	very low	low	very low	high
pH 8 c(NaCl) > 0.3 M	high	none	none	high

Figures

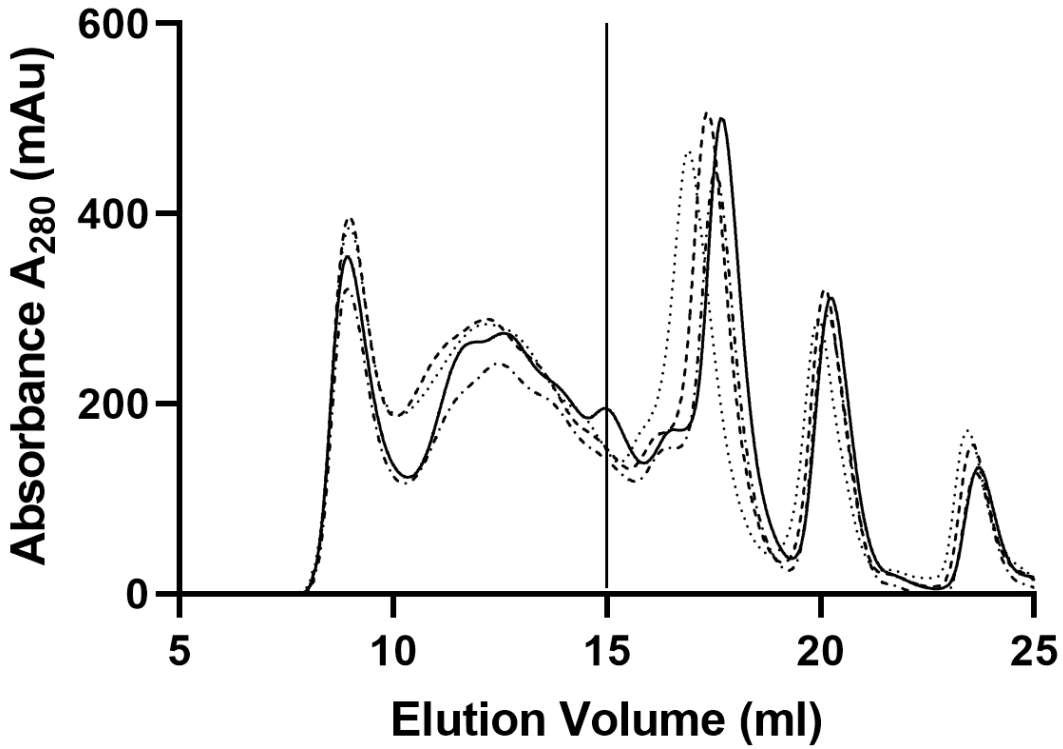

Figure 1. Size exclusion chromatogram of clarified supernatant containing VP1-J8 capsomeres at different NaCl concentrations of the sample. Running buffer had the same composition as the sample. Vertical line indicates the volume (15 ml) at which the capsomeres are expected to elute.
(· · ·) 0.1 M NaCl, (- - -) 0.2 M NaCl, (- · - ·) 0.3 M NaCl, (—) 0.4 M NaCl.

992
993
994
995
996
997
998
999
1000
1001
1002

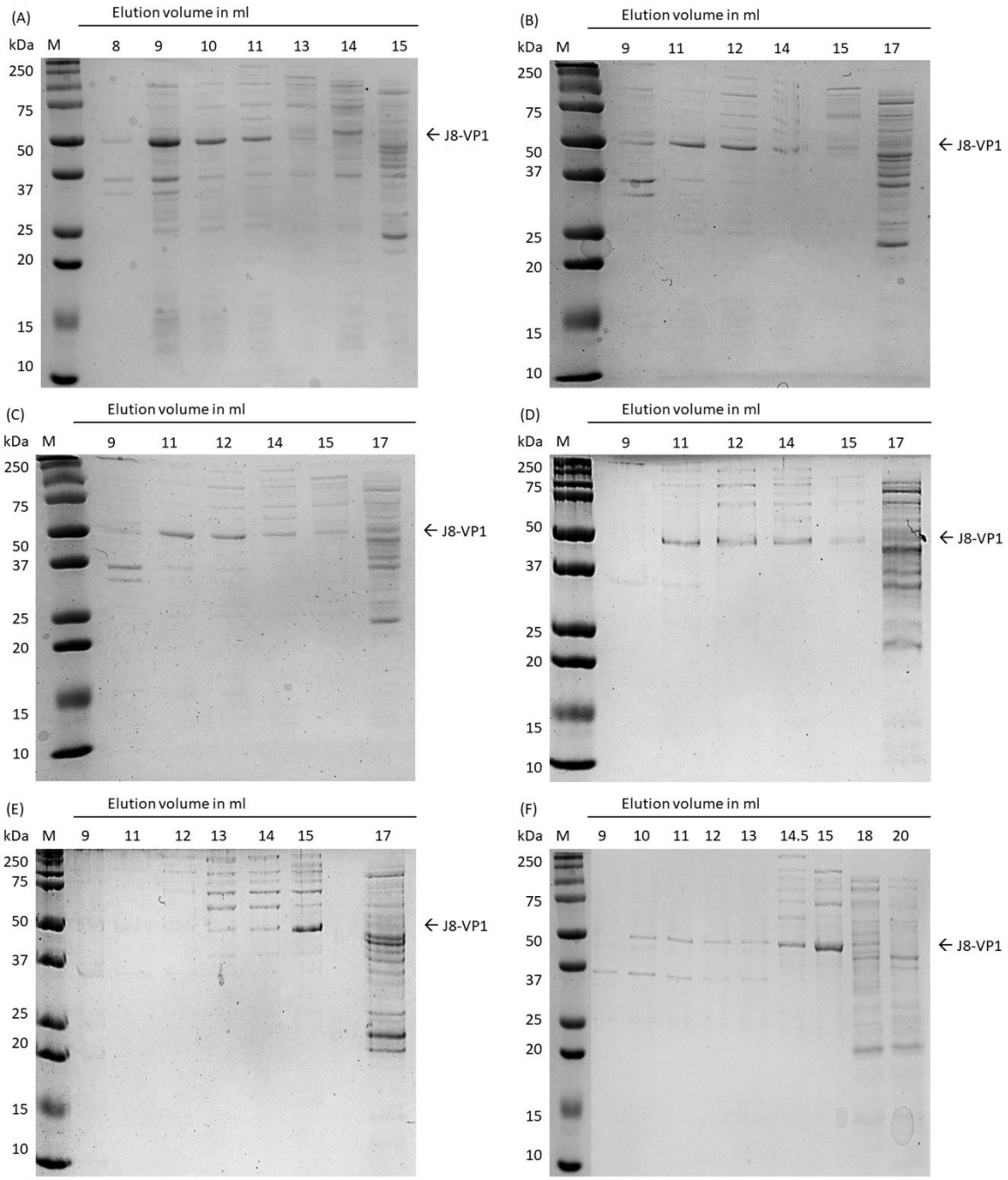

Figure 2. SDS-PAGE analysis of size exclusion fractions of clarified supernatant containing VP1-J8 at different salt concentrations and pH 8. (A) 0 M NaCl, (B) 0.1 M NaCl, (C) 0.2 M NaCl, (D) 0.3 M NaCl, (E) 0.4 M NaCl, (F) 0.5 M NaCl.

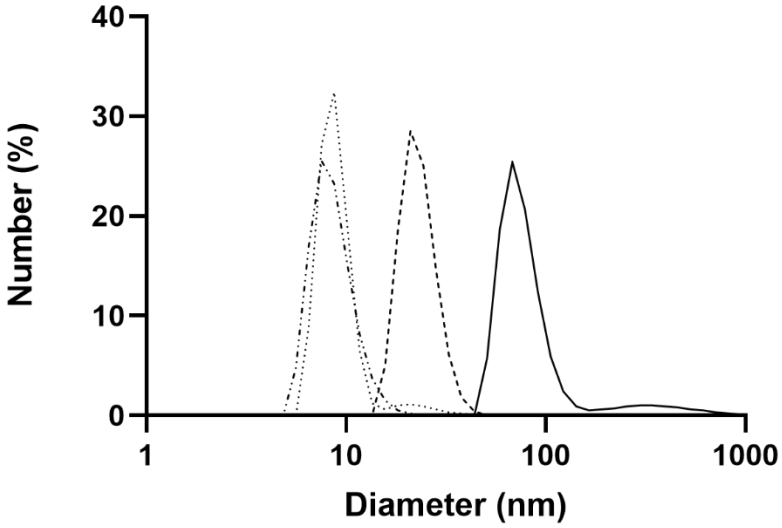

Figure 3. Size distribution of purified VP1-J8 capsomeres with and without DNA measured by dynamic light scattering at different buffer composition. (·····) VP1-J8 in 0.1 M NaCl, (-··-··) VP1-J8 in 0.5 M NaCl, (- - -) DNA in 0 M NaCl (MQW), (—) VP1-J8 + DNA in 0.1 M NaCl.

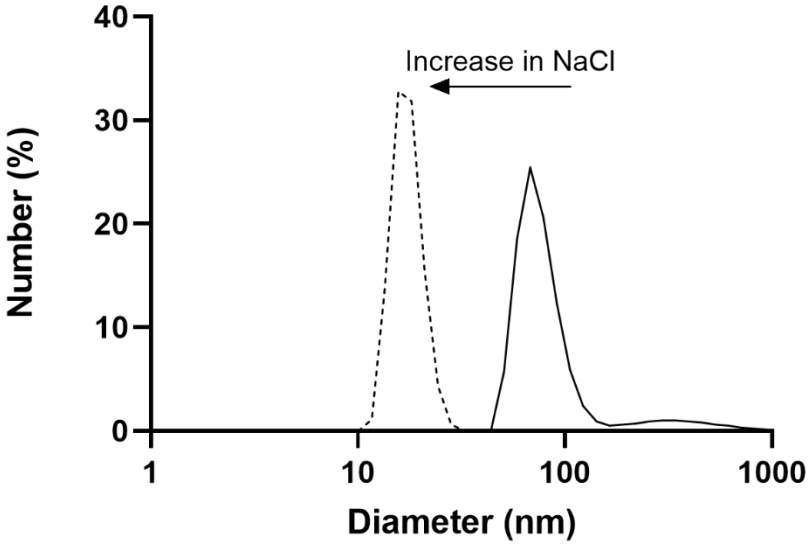

Figure 4. Size distribution of VP1-J8 capsomeres containing DNA, measured by dynamic light scattering, in 0.1 M NaCl (—) and after adding NaCl to a final concentration of 1 M NaCl (- - -).

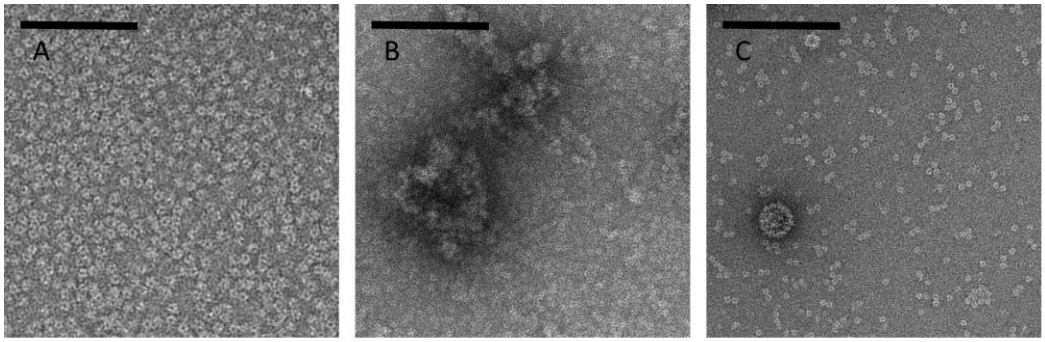

Figure 5. (A) TEM image of purified VP1-J8 capsomeres in 0.1 M NaCl buffer pH 8, containing no DNA. (B) Purified VP1-J8 capsomeres plus unsheared *E.coli* DNA in 0.1 M NaCl buffer pH 8. (C)The same sample as in (B) after the addition of NaCl to a final concentration of 1 M. The scale bar corresponds to 100 nm distance.

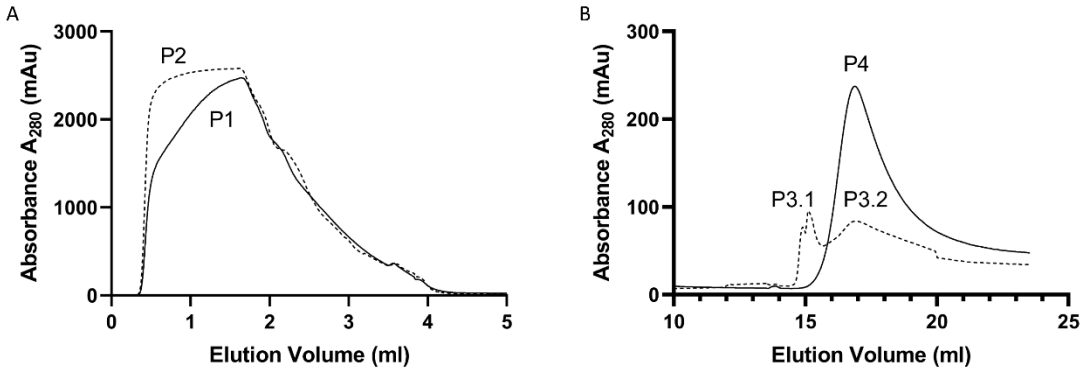

Figure 6. (A) Column loading. Absorbance at 280 nm obtained from the flowthrough while loading 2 ml of resolubilized VP1-J8 (after PEG precipitation) at NaCl concentrations of 0.5 M (—) or 0 M (- --) at pH = 8 onto a 1 ml multimodal weak cation exchanger (Capto™ MMC), loading started at 0 ml (B) Column eluting. Elution profile after loading resolubilized VP1-J8 (after PEG precipitation) at NaCl concentrations of 0.5 M (—) or 0 M (- - -) at pH = 8 onto a 1 ml multimodal weak cation exchanger (Capto™ MMC). Elution was obtained by applying a step gradient of 1 M NaCl phosphate buffer at pH 12 starting at 13.5 ml. The elution buffer had a different absorbance compared to the binding buffer, caused by the instability of DTT, resulting in a baseline shift towards the end of the chromatogram.

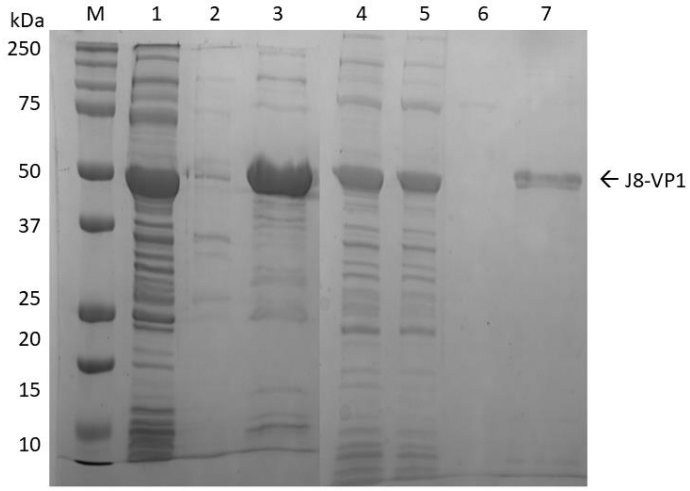

Figure 7. SDS-PAGE analysis of the bind and elute experiments of VP1-J8 onto Capto™ MMC (Figure 6). Lanes (1) & (4) correspond to the starting material used for loading at 0.5 M NaCl (lane 1) and 0 M NaCl (lane 4). (2) Flow through of loading at 0.5 M NaCl (P1 fig. 6a), (3) Elution after loading at 0.5 M NaCl (P4 fig. 6b), (5) Flow through of loading at 0 M NaCl (P2 fig. 6a), (6) First elution peak after loading at 0 M NaCl (P3.1 fig. 6b), (7) Second elution peak after loading at 0 M NaCl (P3.2 fig. 6b).

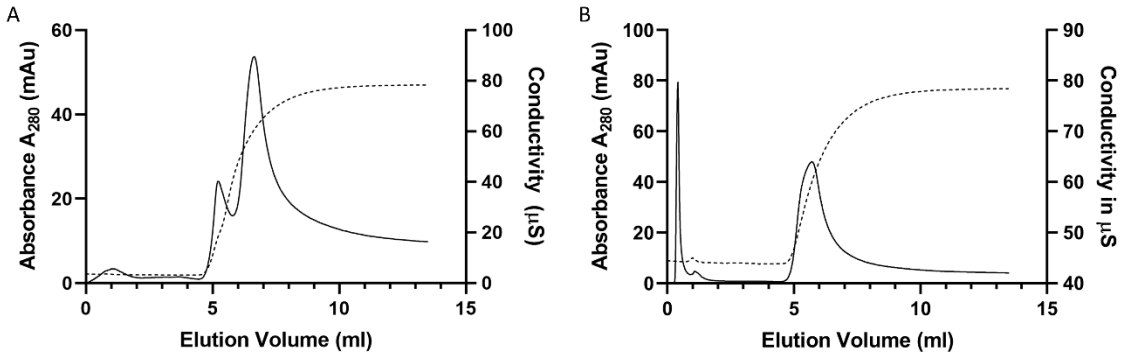

Figure 8. (A) Anion exchange chromatography elution of resolubilized VP1-J8 (after PEG precipitation) loaded on a 1 ml Capto™ Q column at 0.1 M NaCl, pH8. Only a minimal flow through can be observed and most of the protein, including VP1-J8 did bind to the column. VP1-J8 does elute in a first peak at 5ml, followed by a peak of mostly impurities. (—) Absorbance A280, (- - -) Conductivity. (B) Anion exchange chromatography elution of resolubilized VP1-J8 (after PEG precipitation) loaded on a 1 ml Capto™ Q column at 0.5 M NaCl, pH8. VP1-J8 is not binding to the column and remains in the flow through that elutes at 0.5 ml. (—) Absorbance A280, (- - -) Conductivity.

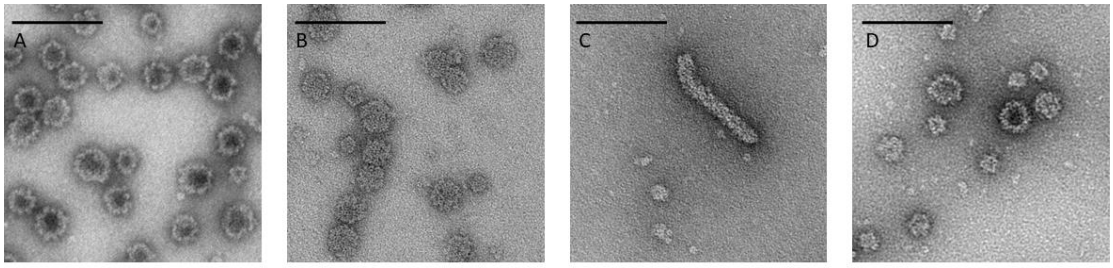

Figure 9. Assembly products of VP1 with and without DNA at different initial NaCl concentrations. Scale bar represents 100 nm. (A) 0.5 M NaCl no DNA. (B) 0.5 M NaCl plus DNA. (C) 0.1 M NaCl plus DNA. (D) 0.1M NaCl no DNA.